Supporting information

Effect of Eutectic Accelerator in Selenium-doped Sulfurized Polyacrylonitrile for High Performance Room Temperature Na-S batteries

Lihui Wang,[ab] Xin Chen,[ab] Shuping Li,[ab] Jiaqiang Yang,[b] Yulong Sun,[a] Linfeng Peng,[a] Bin Shan[b] and Jia Xie*[a]

[a] State Key Laboratory of Advanced Electromagnetic Engineering and Technology, School of Electrical and Electronic Engineering, Huazhong University of Science and Technology, Wuhan 430074, China

[b] State Key Laboratory of Materials Processing and Die & Mould Technology, School of Materials Science and Engineering, Huazhong University of Science and Technology, Wuhan 430074, China

* Address correspondence to xiejia@hust.edu.cn

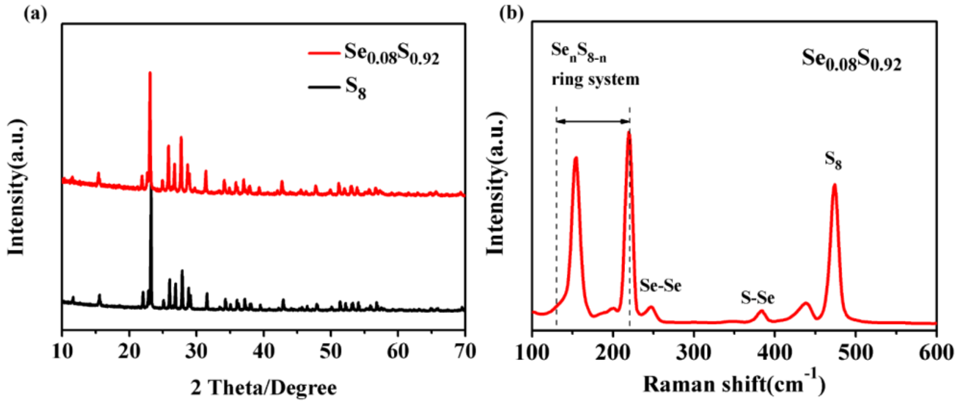

Fig. S1 XRD pattern (a) and Raman spectra (b) of $Se_{0.08}S_{0.92}$.

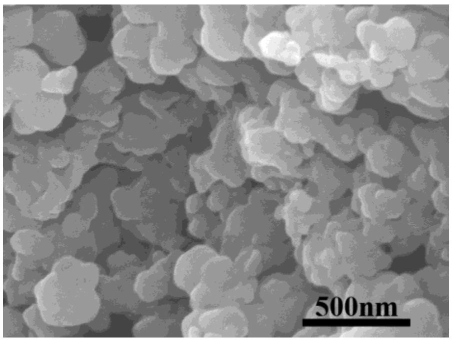

Fig. S2 SEM of S@pPAN

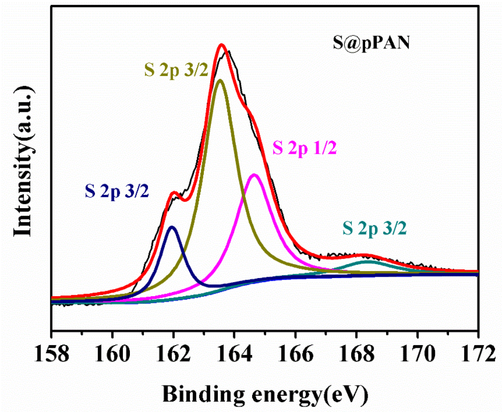

Fig. S3 XPS spectra of S2p for S@pPAN.

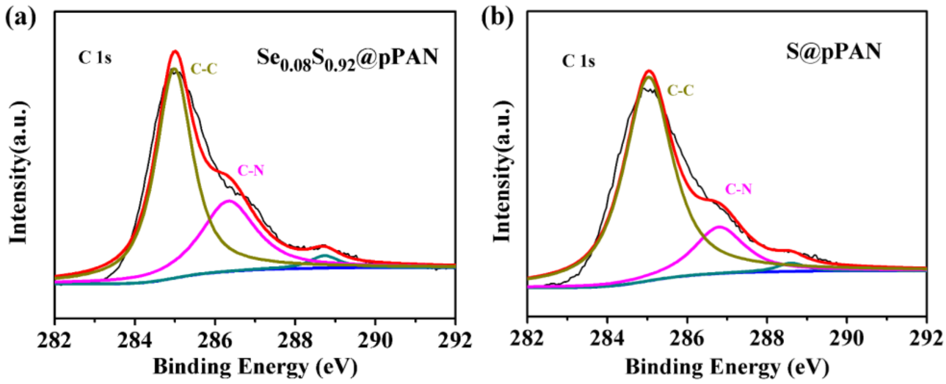

Fig. S4 XPS spectra of C 1s for $Se_{0.08}S_{0.92}$@pPAN (a) and S@pPAN (b).

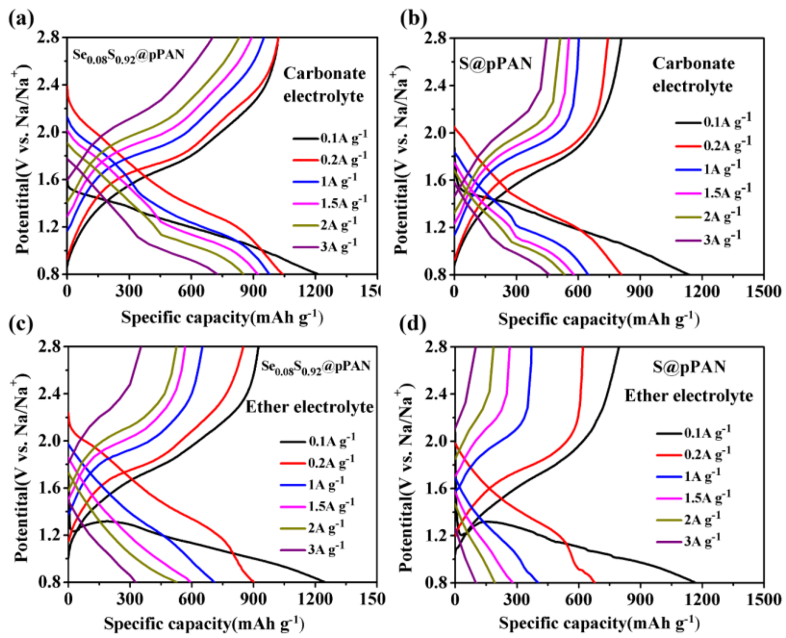

Fig. S5 Voltage profiles at various current densities from 0.1 A g^{-1} to 3 A g^{-1} of $Se_{0.08}S_{0.92}$@pPAN in carbonate electrolyte (a) and in ether electrolyte (c). Voltage profiles at various current densities from 0.1 A g^{-1} to 3 A g^{-1} of S@pPAN in carbonate electrolyte (b) and in ether electrolyte (d).

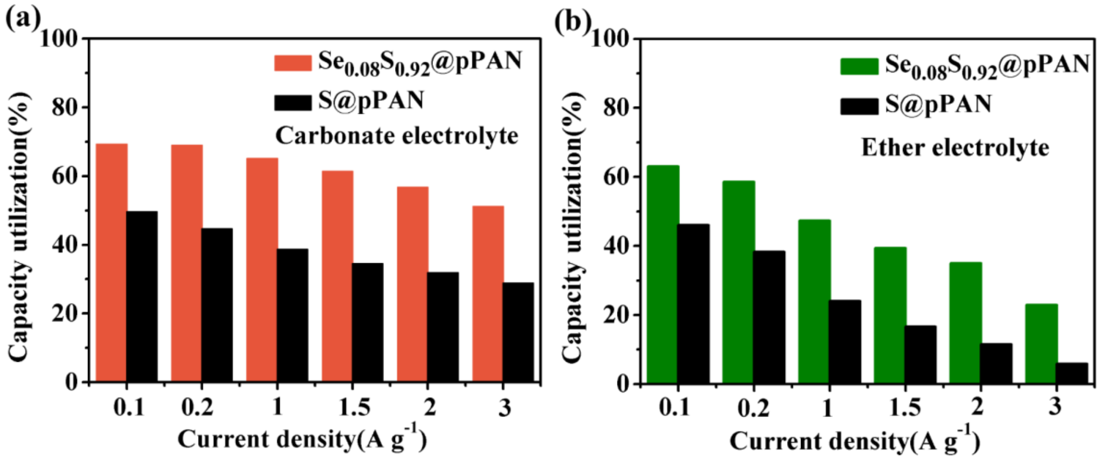

Fig. S6 Comparisions of capacity utilization rates between $Se_{0.08}S_{0.92}$@pPAN and S@pPAN in carbonate electrolyte (a) and in ether electrolyte (b).

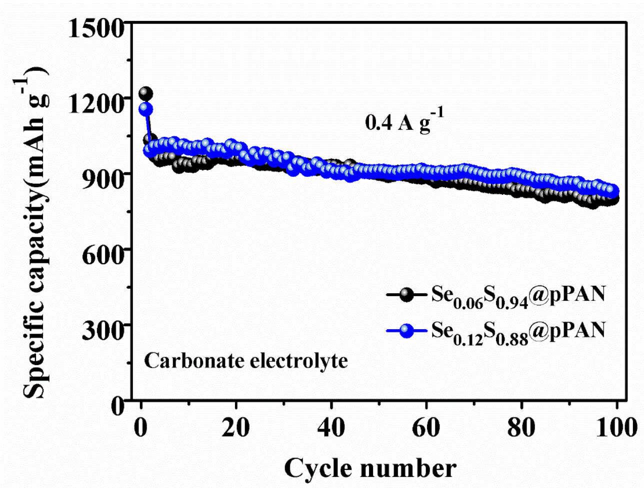

Fig. S7 Cycle performance of $Se_{0.06}S_{0.94}$@pPAN and $Se_{0.12}S_{0.88}$@pPAN composite cathode in carbonate electrolyte.

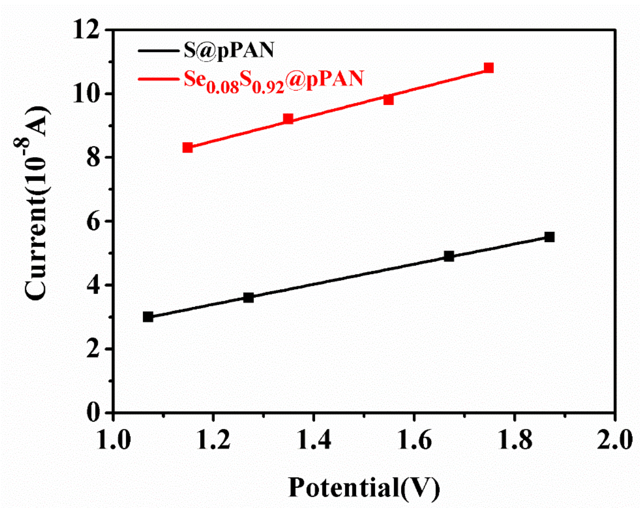

Fig. S8 Equilibrium current of the S@pPAN and $Se_{0.08}S_{0.92}$@pPAN at different set voltages.

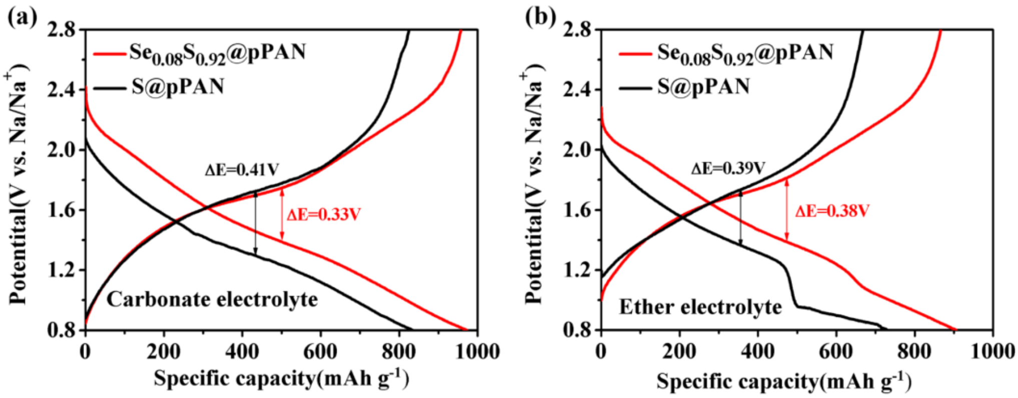

Fig. S9 Discharge/charge curves of $Se_{0.08}S_{0.92}$@pPAN and S@pPAN electrodes in carbonate electrolyte (a) and in ether electrolyte (b).

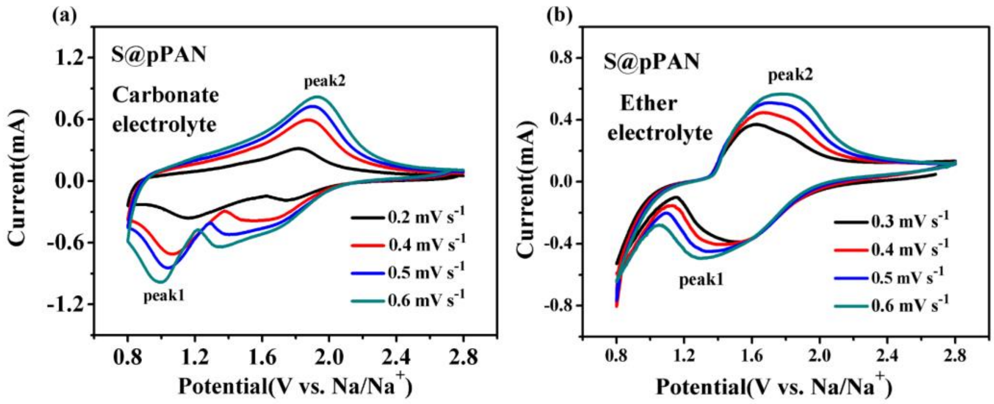

Fig. S10 CV curves of S@pPAN in carbonate electrolyte (a) and in ether electrolyte (b).

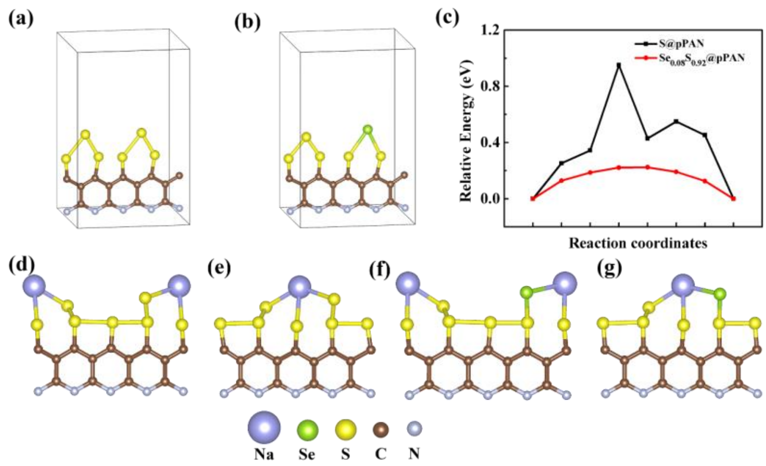

Fig. S11 S@pPAN (a) and $Se_{0.08}S_{0.92}$@pPAN (b) model for Na ion diffusion barriers employing DFT calculation. (c) Energy profiles for Na ion diffusion in S@pPAN and $Se_{0.08}S_{0.92}$@pPAN. Schematic representations of corresponding diffusion pathway for S@pPAN: (d) original state and (e) final state and for $Se_{0.08}S_{0.92}$@pPAN: (f) original state and (g) final state

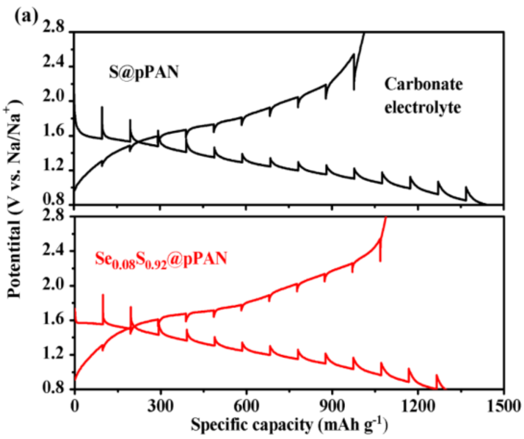

Fig. S12 GITT voltage profiles of the $Se_{0.08}S_{0.92}$@pPAN and of S@pPAN in carbonate electrolyte (a) and in ether electrolyte (b).

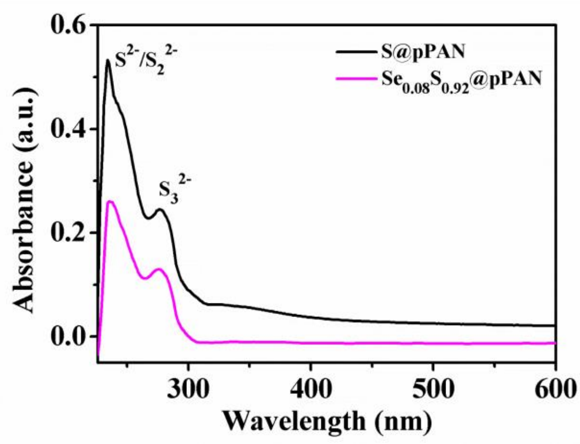

Fig. S13 UV–vis spectra of the S@pPAN and $Se_{0.08}S_{0.92}$@pPAN cathodes solutions cycled in ether electrolyte.

Table S1. The C, N, H, S and Se content in the composite.

Material	C (%)	N (%)	H (%)	S (%)	Se (%)
$Se_{0.06}S_{0.94}$@pPAN	40.5	14.78	0.75	37.78	6.19
$Se_{0.08}S_{0.92}$@pPAN	39.77	14.77	0.85	36.88	7.72
$Se_{0.12}S_{0.88}$@pPAN	40.67	14.99	0.82	32.57	10.97
S@pPAN	41.86	15.56	1	39.35	/

Table S2. Raman shifts (cm^{-1}) and assignments for $Se_{0.08}S_{0.92}$@pPAN.

$Se_{0.08}S_{0.92}$@pPAN	Assignments
307	C-S in plane bending
360	S-Se
470	S-S
805	C-S
926	Ring (containing S-S bond) Stretch
1325	D Band
1532	G Band

Table S3. FTIR wavenumbers (cm^{-1}) and assignments for $Se_{0.08}S_{0.92}$@pPAN.

$Se_{0.08}S_{0.92}$@pPAN	Assignments
1502	C=C Symmetric Stretch
1362	C-C Deformation
1250	C=N Symmetric Stretch
939	Ring Breath (containing C-S)
670	C-S Stretch
513	S-S Stretch

Table S4. Electric conductivity results of S@pPAN and $Se_{0.08}S_{0.92}$@pPAN using direct current (DC) polarization method.

Material	Resistance	Length(cm)	Area(cm^{-2})	Electric conductivity(S/cm)
S@pPAN	3.17×10^7	0.121	0.785	4.86×10^{-9}
$Se_{0.08}S_{0.92}$@pPAN	2.47×10^7	0.113	0.785	5.83×10^{-9}

Table S5. Prolonged cycle life of representative cathodes in carbonate electrolyte for Na-S batteries

Reference	Capacity retention (mAh g^{-1})	Decay rate per cycle (%)
Ref.1	487(500 cycles at 0.7A g^{-1})	0.072
Ref.2	456(200 cycles at 0.5A g^{-1})	0.095
Ref.3	202(160 cycles at 0.5 A g^{-1})	0.214
Ref.4	600(200 cycles at 1.675 A g^{-1})	0.348
Ref.5	292(200 cycles at 0.1A g^{-1})	0.059
Ref.6	256(400 cycles at 3.35 A g^{-1})	0.044
Ref.7	290(350 cycles at 0.1 A g^{-1})	0.288
Ref.8	648(500 cycles at 0.8 A g^{-1})	0.087
(This work)	770(500 cycle at 0.4 A g^{-1})	0.045

References

1. T. H. Hwang, D. S. Jung, J. S. Kim, B. G. Kim and J. W. Choi, *Nano Lett.,* 2013, **13**, 4532-4538.
2. L. Zeng, Y. Yao, J. Shi, Y. Jiang, W. Li, L. Gu and Y. Yu, *Energy Storage Mater.,* 2016**, 5**, 50-57.
3. Y. Yao, L. Zeng, S. Hu, Y. Jiang, B. Yuan and Y. Yu, *Small,* 2017**, 13**, 1603513.
4. S. Xin, Y.-X. Yin, Y.-G. Guo and L.-J. Wan, *Adv. Mater.*, 2014, **26**, 1261-1265.
5. Y. X. Wang, J. Yang, W. Lai, S. L. Chou, Q. F. Gu, H. K. Liu, D. Zhao and S. X. Dou, *J. Am. Chem. Soc.,* 2016, **138**, 16576-16579.
6. G. Xia, L. Zhang, X. Chen, Y. Huang, D. Sun, F. Fang, Z. Guo and X. Yu, *Energy Storage Mater.*, 2018, **14**, 314-323.
7. L. Zhang, B. Zhang, Y. Dou, Y. Wang, M. AlMamun, X. Hu and H. Liu, *ACS Appl. Mater. Interfaces*, 2018, **10**, 20422-20428.
8. X. Xu, D. Zhou, X. Qin, K. Lin, F. Kang, B. Li, D. Shanmukaraj, T. Rojo, M. Armand and G. Wang, *Nat. Commun.*, 2018, **9**, 3870.